Path Following Control for Tracked Vehicles Based on Slip-Compensating Odometry

Daisuke Endo, Yoshito Okada, Keiji Nagatani, and Kazuya Yoshida

Abstract— **Tracked vehicles have the advantage of stable locomotion on uneven terrain, and, as a result, such mechanisms are used for locomotion on outdoor robots, including those used for search and rescue. However, such mechanisms always slip when a tracked vehicle follows a curve, and the slippage generates large accumulated positioning errors in the vehicle compared with conventional wheeled mobile robots. To improve the accuracy of the odometry and enable a path-following control, the estimation of the track slippage is essential. In this paper, we propose an improved method of odometry for tracked vehicles to follow a straight line or a curve. In this method, the vehicle estimates the slip ratios using two encoders (attached to the actuators) and a gyro-sensor. Based on the improved odometry, the path-following control of tracked vehicles is significantly improved. The validity of the method was confirmed with experiments involving our tracked vehicle on several types of surfaces.**

I. INTRODUCTION

Tracked vehicles offer various advantages for locomotion because of their large contact area, which allows them to adapt passively to uneven ground. Therefore, such mechanisms have been used on robotic vehicles designed for search and rescue in disaster areas that might involve operations in collapsed buildings and underground stairs.

We also use tracked vehicles as research platforms for search and rescue in urban disaster environments. In this research, we strive to achieve multi-vehicle remote control from a distant location with a low-bandwidth communication link. In such a case, it is difficult to realize a conventional vision-based remote control (in which an operator controls the robot with a joystick by watching continuous visual information from a camera mounted on the vehicle) because of the low-bandwidth communication. To solve this problem, we are developing another remote control system based on three-dimensional range data and the robot's position [1], [5]. The adoption of autonomous control for tracked vehicles is a particularly important issue, since the maneuverability of the vehicle decreases remarkably due to the time delay and low bandwidth communication.

Therefore, in this research, our objective was to develop a path-following control for tracked vehicles. However, this has been a difficult because "skid-steering" is required. In this method, the turning motion of the vehicle is accomplished by overcoming friction-force between the tracks and the ground. As a result, slippage is generated between the tracks and the ground. Thus, the conventional odometry method to follow a given path for wheeled robots is unreliable when used with tracked vehicles.

To solve this problem, Shiller's group proposed a trajectory-following method for tracked vehicles. They succeeded in implementing a method to follow a given trajectory with consideration of the dynamics of the vehicle in a simulation base[3]. However, their method requires the accurate measurement of the vehicle velocity using internal sensors (e.g., an inertial sensor) and friction coefficients that change depending on the ground surface. In addition, the method is difficult to implement on an actual robot.

To estimate tracked vehicles' position, our approach is based on the estimation of each track's quantitative slippage, which improves the accuracy of the odometry for tracked vehicles. The analysis of the slippage of wheels or track mechanisms is based on the "Theory of Ground Vehicles"[2] (specifically, slip ratio and skid-steering). In [5], we proposed a new odometry method using a gyro-sensor with consideration of the characteristics of the tracked vehicle. The estimation accuracy is better than that with conventional odometry. However, some problems remained with this method. Therefore, in this paper, we propose a new odometry method to improve the accuracy. One of the features of the proposed method is that it can be achieved by a gyro-sensor, encoders (which detect the rotational velocity of tracks), and an empirically identified parameter. The above method was successfully implemented on our tracked vehicle and accurately estimated the position in a real environment. Based on the improved odometry, we also implemented general path-following control (originally used in wheeled vehicles) for tracked vehicles, and validated the performance of the vehicle.

II. ODOMETRY FOR TRACKED VEHICLES

A. Target Vehicles and Conditions

In this research, the following conditions are assumed as target vehicles and surfaces of the ground. A target robot is a tracked vehicle that follows a curve based on skid-steering, and its gravity point is located at the geometric center of its body. Moreover, the vehicle runs in steady-state maneuver, and the contact surface of the left track is nearly identical to that of the right track.

B. Kinematics for Skid-Steering Tracked Vehicles

Odometry is a simple and easy method to estimate the position and orientation of wheeled mobile robots in a pla-

This work has been supported by Strategic Information and Communications R&D Promotion Programme (SCOPE), and New Energy and Industrial Technology Development Organization (NEDO).

D. Endo, Y. Okada, K. Nagatani, K. Yoshida are with Graduate School of Engineering, Tohoku University, Aramaki aza Aoba 6-6-01, Sendai 980-8579, JAPAN keiji@astro.mech.tohoku.ac.jp

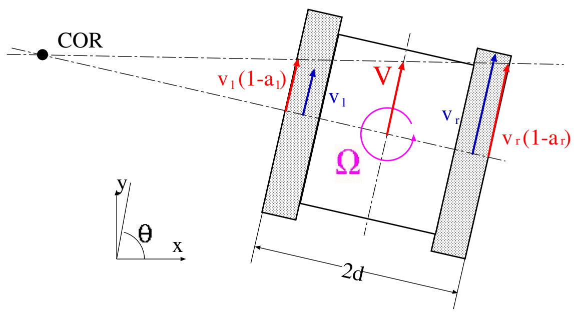

Fig. 1. Kinematic model for tracked vehicles

nar environment. This method requires the assumption that slippage should not be generated between the wheels and the ground. For this reason, it is difficult to apply conventional odometry to tracked vehicles (which slip in a longitudinal direction when the vehicle follows a curve). If the slip ratios of both tracks are detected quantitatively, odometry can be implemented with consideration of the slippage.

To reflect the effects of the slippage, we adopt the following kinematic equations (1)–(3) [2],

$$\dot{x} = \frac{v_r(1-a_r)+v_l(1-a_l)}{2}\cos\theta \tag{1}$$

$$\dot{y} = \frac{v_r(1-a_r)+v_l(1-a_l)}{2}\sin\theta \tag{2}$$

$$\dot{\theta} = \frac{v_r(1-a_r)-v_l(1-a_l)}{2d} \tag{3}$$

where v_l and v_r are, respectively, the theoretical left- and right-track velocities (which are determined from the angular velocities and the radii of the pitch circles of the track's sprockets), $2d$ is the tread. a_l and a_r are the slip ratios defined as,

$$a_l = \frac{v_l - v_l'}{v_l} \tag{4}$$

$$a_r = \frac{v_r - v_r'}{v_r}, \tag{5}$$

where v_l' and v_r' are the absolute velocity of the left and right tracks, respectively. If no slippage occurs, the absolute velocity equals to the theoretical velocity ($v_l' = v_l$, $v_r' = v_r$), and the above equations (1)–(3) result in the conventional kinematics of wheeled mobile robots.

C. Previous Method in [5]

The kinematic equations (1)–(3) show that it is necessary for the realization of the odometry to measure (or estimate) the slip ratios (a_l and a_r). However, slip ratios are determined by physical interactions between the tracks and the ground, and in general, it is difficult to measure the slip ratios directly [5]. Therefore, we assume that the actual angular velocity of the vehicle body, Ω, can be directly measured by a gyro-sensor. Then, we recognize the equation (3) as one of the constraints to estimate a_l and a_r independently; however, another constraint is still required to estimate the slip ratios. In the previous method in [5], we assumed that a_l and a_r were satisfied in the equation (6),

$$\frac{a_l}{a_r} = -\mathrm{sgn}(v_l \cdot v_r), . \tag{6}$$

This condition was intuitively derived from the following characteristics of tracked vehicles:

- When the left and the right tracks rotate in the same direction, the signs of the slip ratios of the left and right tracks are opposite. The slip ratio in a faster rotation is positive and the ratio of the slower one is the negative.
- When the left and the right tracks rotate in the opposite direction, the signs of the slip ratios of the left and right tracks are the same, and both ratios are positive.

Using these conditional equations (3) and (6), a_l and a_r can be obtained. Then, the translational velocity of the vehicle body can be obtained by substitution of the values of slip ratios, a_l and a_r, into the equations (1) and (2), and, finally, the odometry of the tracked vehicle is achieved. When we use the above technique, the odometry accuracy is dramatically improved over that of conventional methods for wheeled mobile robots. However, positioning errors remain, and they tend to increase according to the qualitative increase of the difference between v_l and v_r qualitatively.

D. Proposed Method

In the previous method in [5], one of the problems was the simple assumption (the absolute values of a_l and a_r are always the same) in the equations (6). In actual situations and based on our empirical observation, the slip ratio of the slower track is bigger than the faster one, and the difference of both slip ratios tends to increase according to the qualitatively increase of the difference between v_l and v_r. Therefore, in this research, we assume another new relationship between a_l and a_r, which is shown in the equation (7),

$$\frac{a_l}{a_r} = -\mathrm{sgn}(v_l \cdot v_r)\left|\frac{v_r}{v_l}\right|^n, \tag{7}$$

where n is a specific parameter that may be changed by various factors (track size, tread, and contact characteristics between the track surface and the ground). An identification method of the parameter n is described in Section IV-b.

Once the parameter n is identified, a_l and a_r can be obtained by two conditional equations, (3) and (7). The translational velocity of the vehicle body is obtained by substituting the value of the slip ratios, and the odometry of the tracked vehicle is achieved as well with the previous method in [5]. We refer to this odometry technique as SCOG (Slip Compensated Odometry with Gyro-sensor).

III. EXPERIMENT I

A. Experimental Setup

We conducted various patterns of experiments using our tracked vehicle (CV-04, Technocraft, shown in Fig.2-left) and a motion capture camera (SLC-C02, CyVerse corp.). Figure

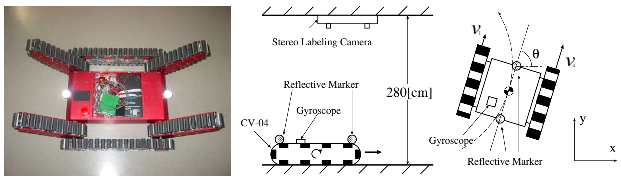

Fig. 2. Tracked vehicle and experimental setup

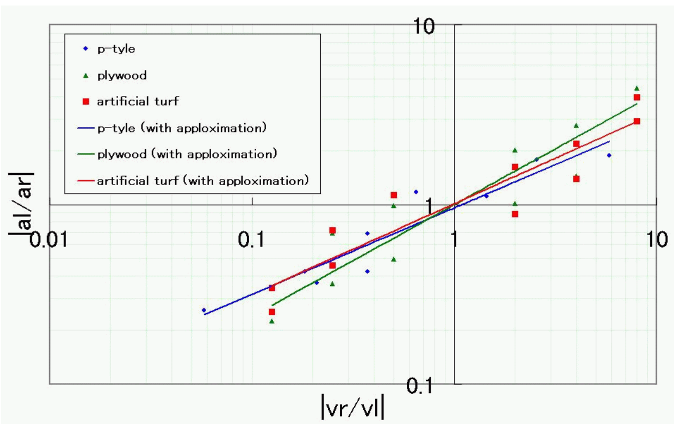

Fig. 3. Results of the parameter n identification experiment

2-right shows an overview of the experimental setup, and TABLE I shows the specifications of this experimental setup.

The vehicle has encoders that measure the left- and right-track velocities. Velocity control of both tracks is performed by general PI feedback. The vehicle also has a rate gyroscope (CRS-03, Silicon Sensing Systems Japan) to detect the angular velocity of the vehicle body. Two markers used to capture the motion, position, and orientation are mounted in the middle of the front and back of the vehicle.

We prepared three types of ground surfaces for experimetal fields: p-tile, plywood, and artificial turf.

B. Identification of n

Using the value of v_l, v_r (detected by the encoders and V) and Ω (detected by the motion capture), the left and right slip ratios (a_l and a_r) are obtained as follows,

$$a_r = 1 - \frac{V + d\Omega}{v_r} \tag{8}$$

$$a_l = 1 - \frac{V - d\Omega}{v_l}. \tag{9}$$

TABLE I

SPECIFICATIONS OF THE EXPERIMENTAL SETUP

Tracked vehicle		Motion capture camera	
Tread	500[mm]	Fixed height	280[cm]
Length of contact area of track	400[mm]	Horizontal accuracy	9[mm]
Total weight	25[kg]	Frame rate	30[fps]
Distance between markers	480[mm]	Base line	400[mm]
Rate gyro's range	0–±100 [deg/sec]	Focal length	3.8[mm]

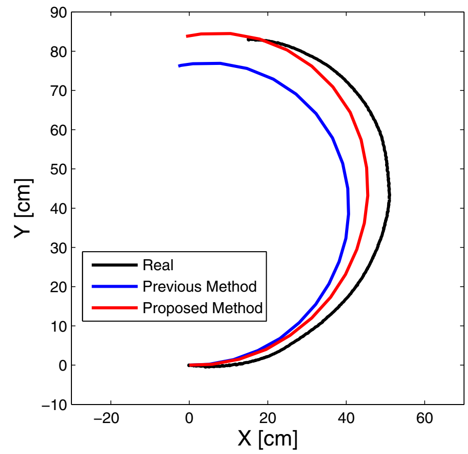

Fig. 4. Real and estimated trajectories of the vehicle following a curve using a p-tyle(at vr = 15.0[cm/sec], vl = 1.9[cm/sec])

We performed various experiments to identify the unknown parameter n in the equation (7) and to verify the change in value by the surface conditions. The results obtained by the different surfaces are shown in Fig.3. The horizontal axis of the logarithmic graph shows $|v_r/v_l|$, and the vertical axis is $|a_l/a_r|$. Parameter n corresponds to the value of the inclination of each line in the graph. Through the use of the least-squares approximation, the parameters obtained were $n = 0.4811$ for p-tyle, $n = 0.6213$ for plywood, and $n = 0.5094$ for artificial turf, respectively. One interesting property is that the parameter n does not change significantly due to the surface when the same tracked vehicle is used in this experiment. Once the parameter n as 0.5 of the CV-04 is approximated, the equation (10) is derived.

$$\frac{a_l}{a_r} = -\text{sgn}(v_l \cdot v_r)\sqrt{\left|\frac{v_r}{v_l}\right|} \tag{10}$$

C. Experimental Result

A set of experimental results, presented in Fig. 4, shows how the estimation accuracy was improved by the proposed SCOG method compared with the previous method in [5]. In this example, where v_l differs widely from v_r, the trajectory estimated by the SCOG method is more similar to the actual trajectory. We performed several sets of similar experiments in which the SCOG method produced more accurate results than the other methods.

Therefore, in conclusion, the accuracy of the odometry for tracked vehicles improves with the use of the SCOG, as proposed in this paper.

IV. PATH FOLLOWING CONTROL OF TRACKED VEHICLES

A. Inverse Kinematics of Skid-Steering Tracked Vehicles

In the case of tracked vehicles, kinematics are described as (1)–(3), which includes the left and right slip ratios. Therefore, the inverse kinematics of tracked vehicles also includes the slip ratios, as follows.

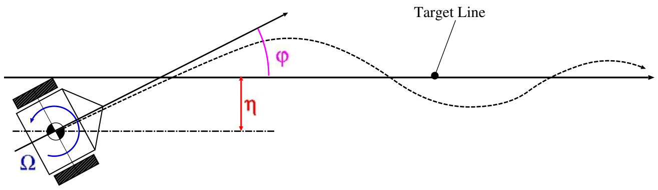

Fig. 5. Image of the control law to make wheeled-type vehicles follow the given target straight line

$$\begin{pmatrix} v_r \\ v_l \end{pmatrix} = \begin{pmatrix} \frac{1}{1-a_r} & \frac{d}{1-a_r} \\ \frac{1}{1-a_l} & -\frac{d}{1-a_l} \end{pmatrix} \begin{pmatrix} V \\ \Omega \end{pmatrix} \tag{11}$$

Equation (11) shows that the target velocities of the vehicle tracks (v_l and v_r) to achieve the target velocity of the vehicle body V and the rotational velocity Ω can not be determined unless the slip ratios (a_l and a_r) are measured or estimated. However, according to the proposed SCOG method, it is possible to estimate the slip ratios (a_l and a_r). Therefore, tracked vehicles are required to follow given paths with conventional control techniques used in general wheeled-type vehicles.

B. Control Law for Following a Straight Line

The control law we adopt for tracked vehicles has been used in most wheeled-type vehicles. Figure 5 shows the control law's image to follow a straight line: φ is the orientation angle between the vehicle body and the target line, and η is the distance between the vehicle body's position and the target line. The line-following motion is achieved by controlling these two variables to 0 by a steering the vehicle. In general, it is well known that the angular velocity Ω of the steering is controlled by the next equation,

$$\left(\frac{d\Omega}{dt}\right)^{ref} = -k_\Omega \Omega - k_\varphi \varphi - k_\eta \eta, \tag{12}$$

where K_Ω, K_φ and K_η are control gains[4].

The above equation shows that the path-following control is achieved when v_l and v_r are controlled on the basis of the equation (11) in order to maintain the reference angular velocity Ω^{ref}, which is calculated using the equation (12). On the other hand, the vehicle translational velocity V^{ref} is always fixed in this method.

C. Control Law for Following a Circuflar Line

When the target path is a circular line, path following is also possible by use of a similar control law. The difference is that the reference straight line of the vehicle should be changed frequently according to the position of the next vehicle (Fig. 6). Details are shown in the following procedure.

1) Set the center point and the radius of the target path of the circular line
2) Figure out the intersection of two lines: one is the target path of the circular line, and the other is the straight line that passes both the center point of the circular line and the robot's present point

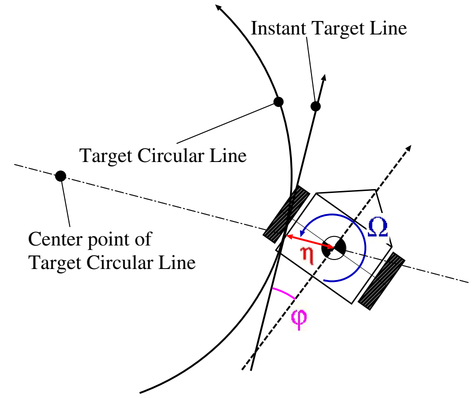

Fig. 6. Image of the control law to make wheeled-type vehicles follow the given target circular line

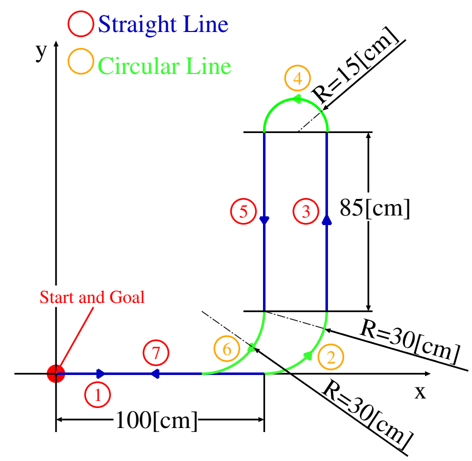

Fig. 7. Target path that consists of a straight line and a circular line

3) Derive the tangent line to the target path of the circular line at the intersection
4) Perform "straight-line following control (in Section IV-B)" to follow the tangent line
5) Repeat the process from 2) to 4)

V. EXPERIMENT II

To verify our path-following method shown in the last section, we conducted experiments using a robot that is identical to that used in Experiment-I and shown in Section III.

A. Setting of the Target Path

The target path set in this experiment is shown in Fig.7. This trajectory consists of 4 straight-line segments and 3 circular-line segments. The tracked vehicle follows the target trajectory by switching the control modes between "straight-line following" (shown in Section IV-B) and "circular-line following" (shown in Section IV-C) to follow straight- or circular-line segments. The switching is executed when location of the vehicle body reaches $1[\mathrm{cm}]$ in the radius range from the final target point of each path.

Details of the vehicle motion are as follows:

1) Departing from the origin (initial point) and then, traveling to 100[cm] along the x axis
2) Turning around in a 30[cm] radius to the left (90[deg]) by following the target circular line which has the center point at $(x, y) = (100, 30)$
3) Going straight from $(x, y) = (130, 30)$ to $(x, y) = (130, 115)$.
4) Turning around in a 15[cm] radius to return (180[deg]) by following the target circular line which has the center point at $(x, y) = (115, 115)$
5) Going straight from $(x, y) = (100, 115)$ to $(x, y) = (100, 30)$.
6) Turning around in a 30[cm] radius to the right (90[deg]) by following the target circular line which has the center point at $(x, y) = (100, 30)$
7) Going back to the origin from $(x, y) = (0, 70)$ along the x axis

It is noteworthy that each track rotates in the same direction in the motion 2) and 6) with a turning radius of $30[\text{cm}]$ and in the opposite direction in the motion 4) with turning radius of $15[\text{cm}]$. This is due to the tread of the CV-04 is $50[\text{cm}]$.

B. Experimental Setup

To measure the actual position and orientation of the vehicle as references, we use the same devices introduced in Section III. We set the target velocity of the vehicle body to a constant value $V^{ref} = 112.8[\text{cm/sec}]$. The surface of the target environment is a flat p-tile floor.

To evaluate the validity of the proposed estimation method, we implemented the conventional odometry used in wheeled-type vehicles and odometry with a gyro for comparison, for comparison purposes. Both conventional methods are summarized as follows:

1) Wheeled-type Odometry: In this method, tracked vehicles are considered to be wheeled-type vehicles, and the slippage of the vehicle tracks is completely disregarded. The translational velocity V and the rotational velocity Ω of the vehicle are represented according to the following equations respectively;

$$V = \frac{v_r + v_l}{2} \tag{13}$$

$$\Omega = \frac{v_r - v_l}{2d}. \tag{14}$$

2) Odometry with a Gyro: In this method, the translational velocity of tracked vehicles V is considered to be similar to that of wheeled-type vehicles, and the rotational velocity Ω is directly sensed by a gyro sensor. The translational velocity V and the rotational velocity Ω of the vehicle are represented according to the following equations respectively;

$$V = \frac{v_r + v_l}{2} \tag{15}$$

$$\Omega = \Omega_{gyro} \tag{16}$$

C. Experimental Results and Discussion

Figure 8, 9, and 10 show three experimental results that display the trajectories of the CV-04 controlled so as to follow the target path on the basis of the three odometry methods. The black line is the target path; the blue line is the estimated trajectory; and the red line is the actual trajectory observed by the motion capture in all graphs.

In all cases, the black lines overlap on the blue lines. This means that the path-following control works well. However, the actual trajectories shown as red lines and detected by the stereo-labeling camera do not line up to the targeted paths. In addition, the size and tendency of these errors have large differences among each set of experiments. In the results based on the wheeled-type odometry, large errors were generated in the orientation angle when the vehicle turned because slippage was not account for. Eventually, the vehicle traveled far from the target path, and stopped at $(x, y, \theta) = (22[\text{cm}], 188[\text{cm}], 2.02[\text{rad}])$. In the result based on the odometry with a gyro, the robot has a small error in the orientation angle. However, the vehicle continued inside of the target paths in its turning motion and stopped at $(x, y, \theta) = (13[\text{cm}], -6[\text{cm}], 3.15[\text{rad}])$. In the result based on the SCOG, the errors were the smallest with the orientation angle and the position in this experiment. Finally, the robot stopped at $(x, y, \theta) = (2[\text{cm}], -3[\text{cm}], 3.15[\text{rad}])$. These results indicate that the odometry with a gyro and SCOG has no difference in principle regarding the accuracy of the orientation angle. However, the actual trajectory based on SCOG is more accurate with the relationship of the given trajectory.

As a consequence, it was verified that the SCOG method performs well with path-following control and conventional control laws.

VI. CONCLUSIONS

In this paper, we proposed an accurate odometry method for tracked vehicles using simple sensors: encoders to detect the velocities of tracks and a gyro-sensor to detect the angular velocity of the tracked vehicle body. A feature of the proposed method, called SCOG, is that it estimates slippage of the tracks by (1) measuring the angular velocity of the vehicle and (2) using a simple assumption of the relationship of each track's slip-ratio, which is obtained empirically. Our experimental results indicated that the SCOG method produces more accurate odometry localization than that achieved with previous methods in [5]. In addition, we applied the SCOG method to path-following control for tracked vehicles, which had been difficult to realize. The experimental results verified that the SCOG performed well with regard to path-following control based on conventional control laws used in wheeled-type robots.

In the SCOG method, we adopted the intuitive equation (7) to estimate the slip ratios. If we describe the relationship between the left and the right slip ratios more accurately and theoretically, the estimation accuracy may be improved. This is one of our important research projects for the future.

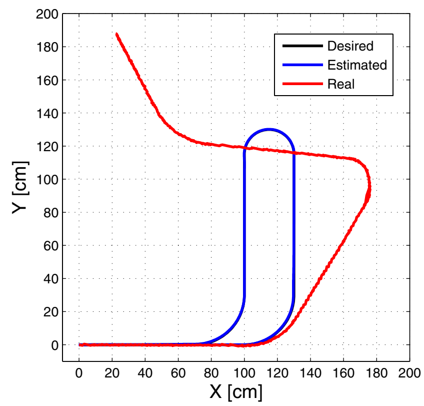

Fig. 8. Results based on "wheeled-type odometry"

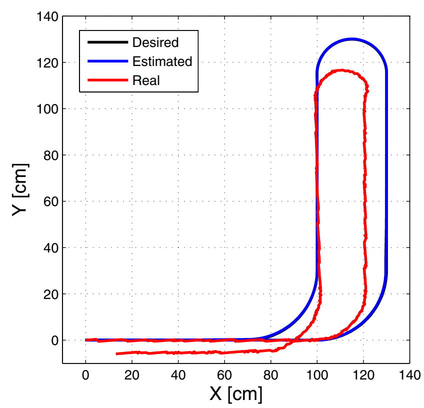

Fig. 9. Results based on "odometry with a gyro"

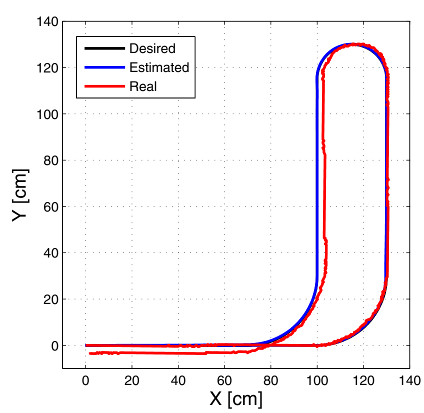

Fig. 10. Results based on "proposed method"

In future work, the above odometry topics will be expanded to slopes and uneven surfaces. In our current forecast, if the center of gravity of a tracked vehicle is close to the geometric center and a the vehicle roll angle is substantially small so as not to generate lateral slippage, the positioning errors would not increase significantly, not even on a slope. That is because the physical interactions (between the tracks and the ground) of the left and right tracks are not different in the case of flat surfaces. Furthermore, in the case of uneven surfaces, the positioning errors would not be expected to increase significantly if the roughness is not too great. This is because, at least, the gyro guarantees a margin of error in the orientation angle, which is more important in odometry to keep accuracy [6]. We will examine some of the questions raised above in real environments in the near future.

VII. ACKNOWLEDGMENTS

The authors gratefully acknowledge the contribution of the Strategic Information and Communications R&D Promotion Program (SCOPE) and the New Energy and Industrial Technology Development Organization (NEDO).

REFERENCES

[1] A. Mora Vargas, K. Mizuuchi, D. Endo, E. Rohmer, K. Nagatani, and K. Yoshida, "Development of a networked robotic system for disaster mitigation -navigation system based on 3d geometry acquisition-", *in Proceedings of the 2006 IEEE International Conference on Robots and Systems*, Beijins, China, 2006.

[2] J. Y. Wong, *Theory of Grond Vehicles*, John Wiley & Sons, 1978.

[3] Z. Shiller and W. Serate, "Trajectory planning of tracked vehicles", *in Transactions of the ASME. Journal of Dynamics Systems, Measurement, and Control*, Vol. 117, pp. 619-624, 1995.

[4] S. Iida and S. Yuta, "Vehicle command system and trajectory control for autonomous mobile robots", *in Proceedings of the 1991 IEEE International Conference on Robots and Systems*, 1991, pp. 212-217.

[5] K. Nagatani, D. Endo and K. Yoshida, "Improvement of the Odometry Accuracy of a Crawler Vehicle with Consideration of Slippage", *in Proceedings of the 2007 IEEE International Conference on Robotics and Automation*, Rome, 2007.

[6] J. Borenstein and L. Feng, "Gyrodometry: A new method for combining data from gyros and odometry in mobile robots", *in Proceedings of the 1996 IEEE International Conference on Robotics and Automation*, 1996, pp. 423-428.